Data in Brief 31 (2020) 105844

Contents lists available at ScienceDirect

Data in Brief

journal homepage: www.elsevier.com/locate/dib

Data Article

Dataset of electrophysiological patch-clamp recordings of the effect of the compounds deltamethrin, ATx-II and β4-peptide on human cardiac Nav1.5 sodium channel gating properties

Sarah Thull[a], Cristian Neacsu[b], Andrias O. O'Reilly[c], Stefanie Bothe[a,d], Ralf Hausmann[e], Tobias Huth[b], Jannis Meents[a,*,**], Angelika Lampert[a,d,f,*]

[a] Institute of Physiology, RWTH Aachen University, Pauwelsstr. 30, 52074 Aachen, Germany
[b] Institut für Physiologie und Pathophysiologie, Friedrich-Alexander-Universität Erlangen-Nürnberg, Universitaetsstr. 17, 91054 Erlangen, Germany
[c] School of Natural Sciences and Psychology, Liverpool John Moores University, Liverpool, United Kingdom
[d] Research Training Group 2416 MultiSenses-MultiScales, RWTH Aachen University, Aachen, Germany
[e] Institute of Clinical Pharmacology, RWTH Aachen University, Wendlingweg 2, 52074 Aachen, Germany
[f] Research Training Group 2415 ME3T, RWTH Aachen University, Aachen, Germany

ARTICLE INFO

Article history:
Received 22 April 2020
Revised 27 May 2020
Accepted 3 June 2020
Available online 08 June 2020

Keywords:
Voltage-gated sodium channel
Human Nav1.5
Sodium channel gating states
Resurgent current
Persistent current
Deltamethrin
ATx-II
β4-peptide

ABSTRACT

This article describes the effect of the pyrethroid insecticide deltamethrin on the cardiac voltage-gated sodium channel Nav1.5. Two concentrations of deltamethrin were used and the effects were compared with those of the sea anemone toxin ATx-II and β4-peptide, which is the C-terminus of the Nav channel β-subunit. Activation, fast inactivation, deactivation, persistent currents and resurgent currents of Nav1.5 channels were assessed in the presence of these compounds. The data display not only the effect of separately applied compounds on Nav1.5 channels but also investigates how combinations of these substances affect Nav1.5 channel gating properties.

DOI of original article: 10.1016/j.taap.2020.115010
* Corresponding author at: Institute of Physiology, RWTH Aachen University, Pauwelsstr. 30, 52074 Aachen, Germany.
** Present address: Multi Channel Systems MCS GmbH, Aspenhaustr. 21, 72770 Reutlingen, Germany.
E-mail addresses: jmeents@multichannelssystems.de (J. Meents), alampert@ukaachen.de (A. Lampert).

https://doi.org/10.1016/j.dib.2020.105844

The dataset presented in this article is related to the research article "Mechanism underlying hooked resurgent-like tail currents induced by an insecticide in human cardiac Nav1.5″ (Sarah Thull, Cristian Neacsu, Andrias O. O'Reilly, Stefanie Bothe, Ralf Hausmann, Tobias Huth, Jannis Meents, Angelika Lampert, doi: 10.1016/j.taap.2020.11501), that investigates the effect of the pyrethroid insecticide deltamethrin on Nav channel gating properties and explains the mechanism underlying hooked, resurgent-like tail currents induced by deltamethrin in Nav1.5 channels.

Specifications Table

Subject	Pharmacology, Toxicology and Pharmaceutics (General)
Specific subject area	Physiology, Biophysics of human Nav channels, Effects of pyrethroid insecticides on human Nav channels
Type of data	Figures
How data were acquired	Whole-cell patch-clamp recordings of Nav1.5 channels expressed in HEK293 cells
Data format	Raw data Analyzed data
Parameters for data collection	Experiments were designed to collect information on the modification of the following parameters by the compounds: i) resurgent-like, hooked tail currents of Nav1.5 ii) kinetics of fast inactivation and deactivation iii) voltage-dependence of activation, persistent and resurgent current, as well as resurgent current kinetics.
Description of data collection	The compounds deltamethrin and ATx-II were applied by incubating the patched cells and β4-peptide was added to the pipette solution. Voltage-protocols were selected to collect data for the parameters indicated above.
Data source location	Institute of Physiology, RWTH Aachen University, Pauwelsstr. 30, 52,074 Aachen, Germany
Data accessibility	Data is provided with the article. Public repository: RWTH Publications, repository number: RWTH-2020-03898.
Related research article	Sarah Thull, Cristian Neacsu, Andrias O. O'Reilly, Stefanie Bothe, Ralf Hausmann, Tobias Huth, Jannis Meents, Angelika Lampert; "**Mechanism underlying hooked resurgent-like tail currents induced by an insecticide in human cardiac Nav1.5**"; Journal of Toxicology and Applied Pharmacology, Under Review

Value of the Data

- The data present the effect of the compounds deltamethrin, ATx-II and β4-peptide on the biophysical properties of human cardiac Nav1.5 channels
- This data are helpful for physiologists and toxicologists interested in Nav channel gating altered by pyrethroid insecticides or sea anemone toxins
- The dataset offers characteristics of the toxicological impact of deltamethrin and ATx-II on human cardiac Nav1.5 channel properties
- The data provide insights into the effect of pyrethroids on β4-peptide induced resurgent currents

Data description

Nav channels are able to produce resurgent currents that are usually generated by an open-channel pore-blocker such as the β4-peptide which unbinds during repolarization [2]. Previous studies report that pyrethroid insecticides induce so-called "hooked tail currents" [6,7]: Nav channels would reactivate during repolarization following a depolarizing voltage step and thereby, form a typical hook, instead of the usually observable single exponential decline of the tail currents [6,7]. Pyrethroids mostly act by slowing deactivation of a pyrethroid-bound Nav channel fraction, thus keeping the channels open and permeable [4,5].

Similar currents as these hooked, resurgent-like tail currents could be observed in Nav1.5 channels treated with 1 µM of the type-II pyrethroid deltamethrin (Sarah Thull, Cristian Neacsu, Andrias O. O'Reilly, Stefanie Bothe, Ralf Hausmann, Tobias Huth, Jannis Meents, Angelika Lampert; "Mechanism underlying hooked resurgent-like tail currents induced by an insecticide in human cardiac Nav1.5″ (Journal of Toxicology and Applied Pharmacology, Under Review). This dataset investigates whether a concentration of 10 µM deltamethrin has the same effect on the human cardiac channel Nav1.5. Analogous to 1 µM deltamethrin, the concentration of 10 µM deltamethrin induced hooked, resurgent-like currents of the same size from a similar repolarization potential of −120 mV to −90 mV (Fig. 1a, b).

In order to investigate the fast gating properties of fast inactivation and deactivation of Nav1.5 channels incubated with 1 µM deltamethrin, the time constants over the first 15 ms of current decay during fast inactivation and deactivation were determined by a double-exponential fit of the current decay as shown in Fig. 2a. The fast time constants of both inactivation and deactivation were not essentially altered. Only τ_{slow} of deactivation in deltamethrin recordings was slower than in vehicle recordings.

ATx-II is believed to stabilize DIV in its deactivated position, thus the inactivation-particle binding site is not formed, and the toxin thereby impedes fast inactivation [3,8,9]. The voltage dependence of Nav1.5 channel activation when treated with 0.5 nM ATx-II and 1 µM deltamethrin did not show a significant difference to recordings with 1 µM deltamethrin and was similar to recordings from untreated cells (Fig. 3a, b). Voltage dependence of activation of 1 µM deltamethrin was slightly left-shifted, activating at more hyperpolarized potentials (Fig. 3b). The combination of ATx-II and deltamethrin produced smaller persistent currents than deltamethrin alone, still showing the same voltage dependence (Fig. 3c). In contrast, the combination of ATx-II and β4-peptide generated smaller persistent currents with a different voltage dependence (Fig. 3c). Large resurgent currents induced by ATx-II and β4-peptide in Nav1.5 channels appeared from −50 mV to −10 mV whereas the hooked, resurgent-like currents evoked by 1 µM deltamethrin could only be observed at very negative potentials from −120 mV to −90 mV (Fig. 3e). With a time-to-peak from approximately 2–4 ms, resurgent-like currents induced by deltamethrin were similar to resurgent currents generated by ATx-II and β4-peptide, arising after approximately 1–5 ms (Fig. 3f).

Resurgent currents induced by the combination of ATx-II, β4-peptide and deltamethrin presented the same voltage dependence as currents evoked by the combination of deltamethrin and β4-peptide, generating currents over the entire voltage range from −120 mV to −10 mV (Fig. 3e). It should be noted that absolute current sizes cannot be compared as the concentration of deltamethrin is tenfold lower in recordings with deltamethrin, ATx-II and β4-peptide than in other recordings. Resurgent currents kinetics from recordings with the triple combination of ATx-II, deltamethrin and β4-peptide were similar to kinetics of the double combination of deltamethrin and β4-peptide, except for an increase in time-to-peak at voltages ranging from −20 mV to 0 mV due to β4-peptide involvement (Fig. 3f).

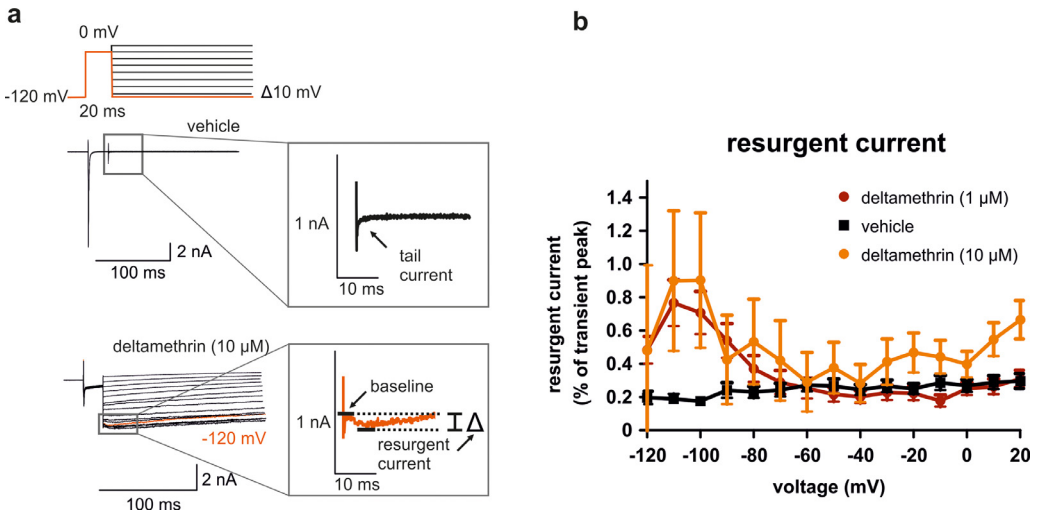

Fig. 1. Nav1.5 channels display resurgent-like currents induced by 10 μM deltamethrin (a) Representative current traces evoked by the indicated voltage protocol in human Nav1.5 channels expressed in HEK293 cells. Cells were treated with vehicle or 10 μM deltamethrin. Representative trace of tail current in vehicle recordings (black) and resurgent-like current at −120 mV of 10 μM deltamethrin (orange) in magnified sections, respectively. Resurgent-like currents were determined as maximal current, elicited after repolarization, subtracted from a baseline. **(b)** Resurgent-like currents were normalized to maximum inward current of the depolarizing pre-pulse. Maximum resurgent-like currents were obtained at −110 mV: 10 μM deltamethrin 0.90% ± 0.42% (yellow, $n = 12$), 1 μM deltamethrin 0.77% ± 0.13% (red, $n = 15$) and vehicle 0.19% ± 0.03% (black, $n = 15$).(For interpretation of the references to color in this figure legend, the reader is referred to the web version of this article.)

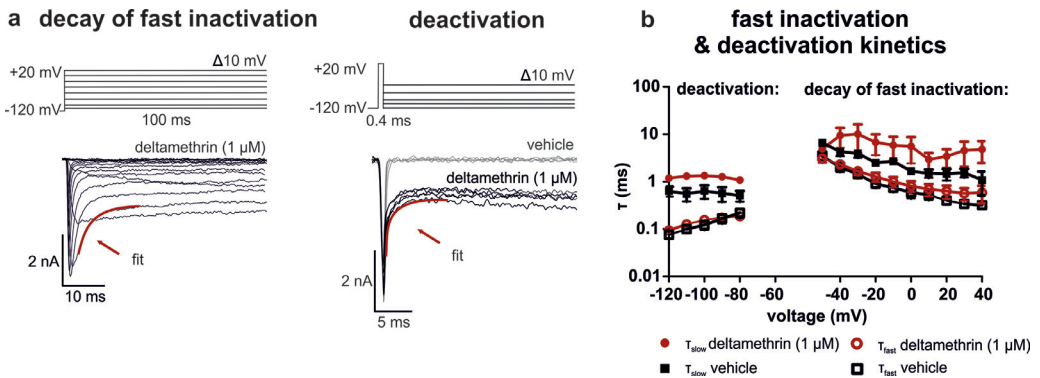

Fig. 2. Time course of fast inactivation and deactivationin deltamethrin unbound Nav1.5 channel**s (a)** Representative voltage protocol and traces of fast inactivation and deactivation kinetics during vehicle (gray) and 1 μM deltamethrin (black) recordings. Time constants of deactivation and fast inactivation were obtained by a double-exponential fit to the current decay, starting very briefly after inward current peak (fit highlighted in red). It should be noted that these fits mainly described the fast component of current decay and thus presumably the fraction of channels that did not bind deltamethrin. **(b)** Mean ± SEM values of the fast time constant (τ_{fast}) and slow time constant (τ_{slow}) of the decay of fast inactivation and deactivation during 1 μM deltamethrin (red) or vehicle (black). Deactivation was depicted from −120 mV to −80 mV, i.e. before the onset of persistent current (see Fig. 4d). For statistical comparison, the area under the curve (AUC) was calculated for each condition: τ_{fast} of 1 μM deltamethrin (unfilled red, $n = 20$, median AUC 0.874×10^{-9} Vs) and vehicle (unfilled black, $n = 13$, median AUC 0.898×10^{-9} Vs, $p > 0.99$, actual difference between the medians $= 0.024 \times 10^{-9}$ Vs, 95.10% CI -0.3×10^{-9} Vs to 0.4×10^{-9} Vs vs. deltamethrin, Mann-Whitney test, no difference to 1 μM deltamethrin), τ_{slow} of 1 μM deltamethrin (filled red, $n = 20$, mean AUC 7.1×10^{-9} Vs) or vehicle (filled black, $n = 8$, mean AUC 5.3×10^{-9} Vs, $p = 0.02$, difference between the means $= 1.8 \times 10^{-9}$ Vs ± 0.7×10^{-9} Vs, 95% CI 0.4×10^{-9} Vs to 3.3×10^{-9} Vs, t-ratio = 2.6 vs. deltamethrin, unpaired *t*-test). The decay of fast inactivation was depicted from −50 mV to +40 mV: τ_{fast} of 1 μM deltamethrin (unfilled red, $n = 10$, median AUC 6.1×10^{-6} Vs) and vehicle (unfilled black, $n = 7$, median AUC 4.4×10^{-6} Vs, $p = 0.03$, actual difference between medians $= 1.7 \times 10^{-6}$ Vs, 95.69% CI 0.2×10^{-6} Vs to 2.4×10^{-6} Vs vs. 1 μM deltamethrin, Mann-Whitney test), τ_{slow} of 1 μM deltamethrin (filled red, $n = 6$, median AUC 37.2×10^{-6} Vs) or vehicle (filled black, $n = 8$, median AUC 18.2×10^{-6} Vs, $p = 0.2$, actual difference between medians $= 19.0 \times 10^{-6}$ Vs, 95.74% CI -11.9×10^{-6} Vs to 48.8×10^{-6} Vs vs. deltamethrin, Mann-Whitney test). As could be predicted from analyzing the deltamethrin unbound channel fraction, fast time constants of both inactivation and deactivation were not essentially altered. Only τ_{slow} of deactivation in deltamethrin recordings is slower than in vehicle recordings. However, as the fits did not include the very slow time course of persistent current decay, these slow time constants presumably describe a mixed population of bound and unbound channels.(For interpretation of the references to color in this figure legend, the reader is referred to the web version of this article.)

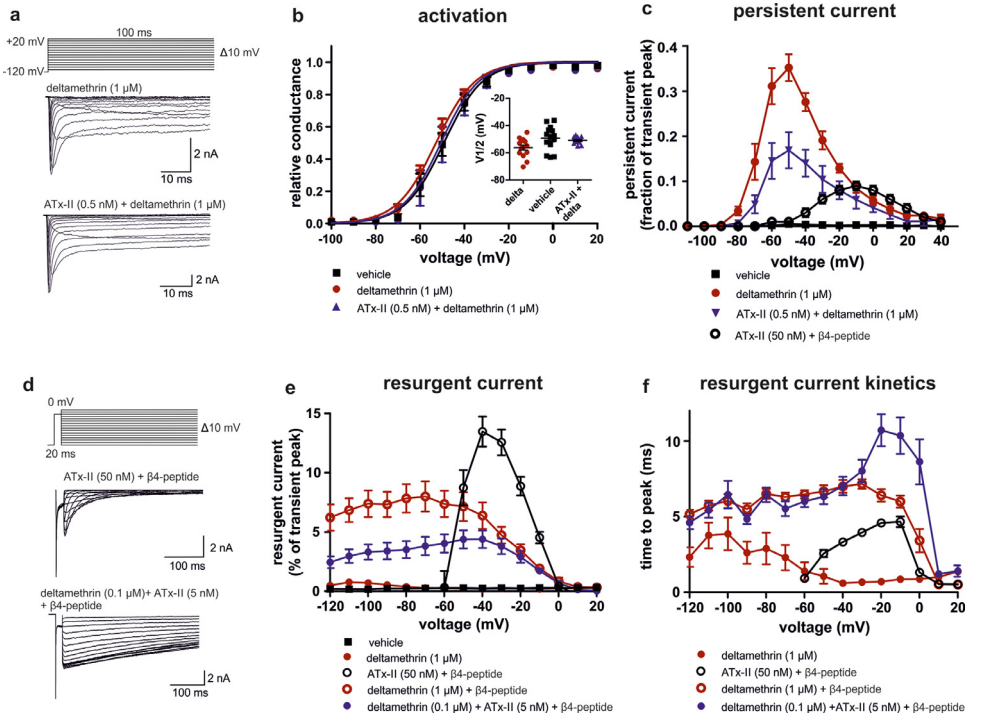

Fig. 3. Effect of ATx-II, deltamethrin and β4-peptide on the gating properties of Nav1.5 channels. (**a**) Representative voltage protocol and current traces of activating sodium currents during 1 μM deltamethrin and 0.5 nM ATx-II +1 μM deltamethrin recordings of Nav1.5 in HEK293 cells. **(b)** Conductance-voltage relationship of Nav1.5 in vehicle, 1 μM deltamethrin or 0.5 nM ATx-II + 1 μM deltamethrin recordings. Conductance was analyzed with leak and zero offset subtraction and normalized to the maximum conductance of each individual cell. Values for half maximal voltage-dependent activation ($V_{1/2}$) were obtained from Boltzmann fits: vehicle −49.2 mV ± 2.4 mV (black, $n = 14$); 1 μM deltamethrin −56.2 mV ± 1.9 mV (red, $n = 14$, $p = 0.03$, difference between means = −7.0 mV ± 2.6 mV, 95% CI −13.6 mV to −0.5 mV, t-ratio = 2.7 vs. Vehicle; $p = 0.2$, difference between means = −5.3 mV ± 2.7 mV, 95% CI −12.1 mV to 1.5 mV, t-ratio = 2.0 vs. 0.5 nM ATx-II + 1 μM deltamethrin); 0.5 nM ATx-II + 1 μM deltamethrin −50.9 mV ± 0.8 mV (blue, $n = 12$, $p > 0.99$, difference between means = 3.4 mV ± 2.7 mV, 95% CI −5.1 mV to 8.5 mV, t-ratio = 0.6 vs. vehicle, one-way ANOVA with a Bonferroni's post-hoc analysis). Conductance of ATx-II + deltamethrin recordings shows no difference to vehicle recordings. **(c)** Mean persistent current was obtained during the final 13 ms of 100 ms depolarizing pulses in vehicle, 1 μM deltamethrin, 0.5 nM ATx-II + 1 μM deltamethrin and 50 nM ATx-II + 100 μM β4-peptide. Currents were analyzed with leak and zero offset subtraction and normalized to the maximum inward current. Maximum persistent currents at −50 mV, evoked by vehicle 0.01 ± 0.00 (black, $n = 19$), 1 μM deltamethrin 0.35 ± 0.03 (red, $n = 24$) or 0.5 nM ATx-II + 1 μM deltamethrin 0.17 ± 0.04 (blue, $n = 12$), and at 0 mV, evoked by 50 nM ATx-II + 100 μM β4-peptide 0.08 ± 0.01 (unfilled black, $n = 14$). The combination of ATx-II and deltamethrin and ATx-II and β4-peptide generates smaller persistent currents than deltamethrin alone. Also note the different voltage dependence of ATx-II + β4-peptide persistent currents. **(d)** Representative resurgent current traces evoked by the indicated voltage protocol recorded in 50 nM ATx-II + 100 μM β4-peptide and 0.1 μM deltamethrin + 5 nM ATx-II + 100 μM β4-peptide recordings in Nav1.5 channels. **(e)** Resurgent currents were determined and analyzed as in Fig. 2a (gray box) and normalized to the maximum inward current of the depolarizing pre-pulse. Resurgent currents evoked by vehicle (black, $n = 16$); 1 μM deltamethrin (filled red, $n = 16$); 50 nM ATx-II + 100 μM β4-peptide (unfilled black, $n = 15$); 1 μM deltamethrin + 100 μM β4-peptide (unfilled red, $n = 13$); and 0.1 μM deltamethrin + 5 nM ATx-II + 100 μM β4-peptide (filled blue, $n = 17$). ATx-II and β4-peptide resurgent currents were depicted from −60 mV since the combination does not produce resurgent currents at more negative potentials [1]. Resurgent currents of combinations including β4-peptide are generally larger than deltamethrin-induced resurgent-like currents. Note the different voltage dependence of ATx-II and β4-peptide resurgent currents. Also note the tenfold smaller deltamethrin concentration of the combination of ATx-II + deltamethrin + β4-peptide (filled blue circles) compared to previous measurements. **(f)** Time-to-peak of the resurgent current was measured in individual recordings and plotted against the repolarization voltage: 1 μM deltamethrin (filled red, $n = 20$), 50 nM ATx-II + 100 μM β4-peptide (unfilled black, $n = 15$), 1 μM deltamethrin + 100 μM β4- peptide (unfilled red, $n = 17$), 0.1 μM deltamethrin + 5 nM ATx-II + 100 μM β4-peptide (blue, $n = 19$). Resurgent-like currents induced by either deltamethrin or β4-peptide alone are generally faster than those induced by combinations including deltamethrin and β4-peptide.(For interpretation of the references to color in this figure legend, the reader is referred to the web version of this article.)

Experimental design, materials, and methods

Methods are partially identical to those published in Sarah Thull, Cristian Neacsu, Andrias O. O'Reilly, Stefanie Bothe, Ralf Hausmann, Tobias Huth, Jannis Meents, Angelika Lampert; "Mechanism underlying hooked resurgent-like tail currents induced by an insecticide in human cardiac Nav1.5″; Journal of Toxicology and Applied Pharmacology, doi: 10.1016/j.taap.2020.11501.

Cell culture and transfection

A HEK293 cell line stably expressing hNav1.5 was used and cultivated using DMEM/ F-12 medium (Gibco-Life technologies) with added 10% FBS, 1% Penicillin/Streptomycin (A&E Scientific). Incubation of cells was performed at 5% CO_2 and 37 °C.

Chemicals

Unless otherwise stated, chemicals were acquiredaquired from Merck (Germany) or Sigma (Germany). For the β4-peptide (sequence 'KKLITFILKKTREK', PSL GmbH), a stock solution was prepared in water. To reach the final concentration of 100 μM the stock solution was diluted in internal solution right before experiments. The diluted β4-peptide was kept at 4 °C.

Recombinant ATx-II (Anemonia sulcata toxin, Alomone Labs, Jerusalem, Israel or Sigma-Aldrich, USA) was prepared as a stock solution in water, which was then diluted in extracellular solution to produce a final concentration of 5 nM. A stock solution of deltamethrin (Sigma-Aldrich, USA) in DMSO was diluted in extracellular solution to a final concentration of 1 µM, yielding a final DMSO concentration of maximum 0.1%. This DMSO concentration had no effect on Nav1.5 sodium currents. Cells were treated with vehicle (0.1% DMSO) in bath solution for control conditions.

Electrophysiology

HEK293 cells were recorded at room temperature (22 ± 1 °C) using an EPC 10 USB patch-clamp amplifier (HEKA Electronics, Germany). Sampling rate was set to 100 kHz while using a 10 kHz low-pass filter (for recordings of recovery of fast inactivation and resurgent current a 50 kHz sampling rate was used).

Recording patch pipettes manufactured with a DMZ puller (Zeitz Instruments GmbH, Martinsried, Germany) had a tip resistance between 0.9 and 2.5 MΩ. Bath solution contained the following (in mM): 140 NaCl, 3 KCl, 1 $MgCl_2$, 1 $CaCl_2$, 10 HEPES, 20 Glucose (pH 7.4, adjusted with NaOH). Patch pipette solution was (in mM): 140 CsF, 10 NaCl, 10 HEPES, 1 EGTA, 18 Sucrose (pH 7.33, CsOH). ß4-peptide was diluted in internal solution to a final concentration of 100 μM for some experiments.

Series resistance was compensated by at least 65%. Leak current was subtracted online with the P/4 procedure. Recordings were performed in whole-cell configuration using PatchMaster-Patchmaster software (HEKA Elektronik, Lamprecht, Germany) and analyzed by FitMaster software (HEKA Elektronik, Lamprecht, Germany). Sodium currents were allowed to stabilize during 3 min before start of the recording. V_{hold} was set to −120 mV.

100 ms pulses were used to measure current-voltage (I–V) relations and various potentials in 10 mV steps were applied with an interpulse interval of 5 s. Conductance G_{Na} was defined as: $G_{Na} = I_{Na}/(V_m - V_{rev})$ with I_{Na} as the amplitude at the voltage V_m, and the reversal potential for sodium being V_{rev}, which was determined for each cell individually. For each individual cell, conductance was normalized to the maximum conductance. Normalized conductance ($G_{Na}/G_{Na,max}$) was plotted as a function of test potential. The following Boltzmann equation was used to fit

activation curves: $G_{Na}/G_{Na,max} = G_{Na,\ max}/(1 + \exp\ [(V_m - V_{1/2})/k])$ with $G_{Na,\ max}$ as the maximum sodium conductance, $V_{1/2}$ the membrane potential at half-maximal channel activation, the membrane voltage V_m and the slope factor *k*.

The final 13 ms of a 100 ms depolarizing pulse from −120 mV to +20 mV were used to assess mean persistent current. The maximum current, elicited by the depolarizing pre-pulse, was used to normalize current amplitude.

For resurgent current investigation, we used a 20 ms depolarizing pre-pulse to 0 mV to open the channel and allow a pore blocker to bind. The following 500 ms test-pulse in steps of 10 mV (ranging from −120 mV to +20 mV) with deltamethrin in the bath and in some experiments with the β4-peptide in the internal solution or ATx-II in the external solution was used to measure resurgent currents. To investigate even very small resurgent currents, analysis was performed without leak subtraction. By subtracting the maximum resurgent current from a baseline which was defined as shown in Fig. 1a, absolute currents were analyzed. Resurgent currents were normalized to the maximum inward current, elicited by the depolarizing pre-pulse. By measuring the time-to-peak of the resurgent current at the beginning of the repolarizing pulse, we assessed resurgent current kinetics.

Voltage-dependence of steady-state fast inactivation was measured with a two-pulse protocol. First, a series of 500 ms pre-pulses ranging from −150 mV to −10 mV in steps of 10 mV was applied, then a 40 ms depolarization to +20 mV served as a test-pulse to assess the available non-inactivated channels. Relative currents were calculated as test-pulse currents at each voltage divided by the maximum inward current during the test-pulse of one recording series ($I_{Na}/I_{Na,\ Max}$). Relative currents were fitted with the above Boltzmann equitation, G_{max} was set to 1.

For investigation of deactivation, a 0.4 ms depolarizing pre-pulse to +20 mV was applied, followed by a repolarization from −120 mV to +20 mV in 10 mV steps. The fast component of current decay of fast inactivation and deactivation during the first 15 ms of current decay was fitted by a double-exponential equation: $Y = Y_0 + A_{fast}{}^{*}\exp(-K_{fast}{}^{*}X) + A_{slow}{}^{*}\exp(-K_{slow}{}^{*}X)$, with Y_0 as the current amplitude at steady-state (i.e. plateau), A_{fast} and A_{slow} being the amplitude coefficient for the fast and the slow time constants, and K_{fast} and K_{slow} representing the two rate constants, while X is the time. The reciprocals of the respective rate constant K reveal the time constants τ_{fast} and τ_{slow}. Leak subtraction was omitted as well as zero offset subtraction during analysis of current decay (fast inactivation). This measure helped to reduce the impact of deltamethrin-altered leak currents on our recordingsrecrodings.

Data analysis and statistics

More than two groups were compared for statistical analysis by an ANOVA or a Kruskal-Wallis test in case of non-Gaussian distribution, which was then followed by a Bonferroni, Dunnett or Dunn post-hoc analysis. A student's *t*-test for parametric testing or a Mann Whitney test for non-parametric testing was used to compare two groups. We assumed significance if $p \leq 0.05$. We specified the significance level by the 95% confidence interval, the difference between the means and t-ratio (difference between sample means divided by the standard error of the difference) for parametric testing or actual difference between medians and 95.10%, 95.69% or 95.74% confidence interval (Fig. 2) for non-parametric testing. Grubb's test (Graph pad QuickCalcs) was used to investigate exponential fits and area under the curve (AUC) data for significant outliers and those identified were excluded from analysis.

Declaration of Competing Interest

The authors declare that they have no known competing financial interests or personal relationships which have, or could be perceived to have, influenced the work reported in this article.

Acknowledgments

The authors thank Petra Hautvast and Brigitte Hoch for excellent technical assistance. The authors declare no competing financial interests. This work was supported in part by the DFG LA 2740/3–1, the DFG-funded research training groups 363055819/GRK2415 and 368482240/GRK2416 (all to A.L.) and by a grant from the Interdisciplinary centre for Clinical Research within the faculty of Medicine at the RWTH Aachen University (IZKF TN1–8/IA 532008).

This data in brief article is associated with: Sarah Thull, Cristian Neacsu, Andrias O. O'Reilly, Stefanie Bothe, Ralf Hausmann, Tobias Huth, Jannis Meents, Angelika Lampert; Mechanism underlying hooked resurgent-like tail currents induced by an insecticide in human cardiac Nav1.5, Journal of Toxicology and Applied Pharmacology (2020), doi: 10.1016/j.taap.2020.11501.

References

[1] A.H. Lewis, I.M. Raman, Interactions among DIV voltage-sensor movement, fast inactivation, and resurgent Na current induced by the NaVβ4 open-channel blocking peptide, J. Gen. Physiol. 142 (2013) 191–206.
[2] I.M. Raman, B.P. Bean, Resurgent sodium current and action potential formation in dissociated cerebellar Purkinje neurons, J. Neurosci. Off. J. Soc. Neurosci. 17 (1997) 4517–4526.
[3] N. el-Sherif, H.A. Fozzard, D.A. Hanck, Dose-dependent modulation of the cardiac sodium channel by sea anemone toxin ATXII, Circ. Res. 70 (1992) 285–301.
[4] D.M. Soderlund, State-dependent modification of voltage-gated sodium channels by pyrethroids, Pestic. Biochem. Physiol. 97 (2010) 78–86.
[5] D.M. Soderlund, Molecular mechanisms of pyrethroid insecticide neurotoxicity: recent advances, Arch. Toxicol. 86 (2012) 165–181.
[6] J.H. Song, T. Narahashi, Modulation of sodium channels of rat cerebellar Purkinje neurons by the pyrethroid tetramethrin, J. Pharmacol. Exp. Ther. 277 (1996) 445–453.
[7] H. Tatebayashi, T. Narahashi, Differential mechanism of action of the pyrethroid tetramethrin on tetrodotoxin-sensitive and tetrodotoxin-resistant sodium channels, J. Pharmacol. Exp. Ther. 270 (1994) 595–603.
[8] H. Vais, M.S. Williamson, S.J. Goodson, A.L. Devonshire, J.W. Warmke, P.N. Usherwood, C.J. Cohen, Activation of Drosophila sodium channels promotes modification by deltamethrin. Reductions in affinity caused by knock-down resistance mutations, J. Gen. Physiol. 115 (2000) 305–318.
[9] J.W. Warmke, R.A.G. Reenan, P. Wang, S. Qian, J.P. Arena, J. Wang, D. Wunderler, K. Liu, G.J. Kaczorowski, L.H.T.V. der Ploeg, B. Ganetzky, C.J. Cohen, Functional Expression of drosophila para sodium channels : modulation by the membrane protein TipE and toxin pharmacology, J. Gen. Physiol. 110 (1997) 119–133.